

Mesoscopic linear alignment and thermal-relaxation dynamics of aggregated gold nanorods

O.-H. Kwon, S. Lee, and D.-J. Jang^a

School of Chemistry, Seoul National University, NS60, Seoul 151-742, Korea

Received 6 September 2004

Published online 13 July 2005 – © EDP Sciences, Società Italiana di Fisica, Springer-Verlag 2005

Abstract. Aqueous gold nanorod colloids aggregated by Cl^- are further assembled into linearly aligned structures of linear bundles during evaporation on TEM grids. Gold nanorods in bundles are also oriented in nearly head-to-tail shapes in the microscopic scale. Induced dipolar long-range interactions in the mesoscopic scale are suggested to drive gold nanorods to aggregate. Although surface-plasmon absorption at transverse resonances decreases, that at longitudinal resonances increases with aggregation. The photon-thermalized heat of the dispersed and the aggregated gold nanorods dissipates to immediately surrounding media on the time scales of 100 and 800 ps, respectively.

PACS. 81.16.-c Methods of nanofabrication and processing – 78.67.-n Optical properties of low-dimensional, mesoscopic, and nanoscale materials and structures – 81.07.-b Nanoscale materials and structures: fabrication and characterization

1 Introduction

Extensive recent research has been directed toward the organization of chemical assemblies in nanoscale dimensions [1–11]. The adsorption of nanometer-size particles from colloidal suspensions onto substrates [5–7] and the organization of nanomaterials in two- or three-dimensional assemblies [8, 12] represent current active fields of research in colloid and surface sciences. Beyond the fundamental motivation to understand the underlying mechanisms involved in self-organization processes, self-assembled architectures of metallic nanoparticles have potential applicabilities in nanotechnologies [7, 13]. Irrespective of their specific applications, the ultimate properties of nanostructures are critically determined by their topology and length scale [14, 15]. Therefore, the control of the ordering of nanoparticles appears most important for both templated architectures and functional devices.

The phenomena of aggregation and flocculation by cross-linking agents in gold colloidal solutions are well reported [16, 17]. Attempts to control the aggregation processes have been centered on carboxylate-functionalized colloids, which display flocculation behaviors as a function of pH [7]. Although these colloids are stable at high pHs, they aggregate at low pHs owing to protonated carboxylic functions allowing inter-particle interactions. These aggregates can often be re-dispersed by increasing pH. Similar reversible aggregation can also be observed in DNA-coated colloids [18, 19], for which the transition temperature of

particles to aggregates is indicative of the complementary degree of DNA.

Spherical gold nanoparticles show strong surface-plasmon absorption in the visible region of 520 nm resulting from the resonant oscillations of free electrons in the conduction band. However, the plasmon resonances split into two modes, longitudinal and transverse, for gold nanorods. The longitudinal mode is very sensitive to the ratio of length to diameter (aspect ratio), shifting to the red with the increase of the aspect ratio [6]. The flocculation of gold nanoparticles also leads to the appearance of new absorption near longitudinal resonances. The close contact of nanoparticles having surface-plasmon resonances brings in new absorption bands attributed to the coupling of the plasmon resonances. The induced aggregation of nanoparticles by ions has attracted researchers to reveal the underlying mechanisms of salt effects [5, 6]. Two mechanisms are reported to cause the aggregation of spherical nanoparticles [6]. Multiply charged aggregants can bind nanoparticles together into dense aggregates to display absorption around 700 nm. On the other hand, singly charged ones cause slow aggregation to produce string-like aggregates having less defined absorption [6].

We report in this paper that aqueous gold nanorod colloids aggregated by Cl^- form linearly aligned structures of linear bundles during evaporation on carbon-coated copper TEM grids. Induced dipole-dipole long-range interactions are suggested to drive gold nanorods to flocculate with mesoscopic linearity. Our transient-absorption study shows that whereas the excitation-thermalized heat

^a e-mail: djjang@plaza.snu.ac.kr

of gold nanorods dissipates within 100 ps, that of aggregates does on the slow time scale of 800 ps.

2 Experimental

Gold nanorods having an average diameter of 7 nm with an average aspect ratio of 4 were prepared by the previously described electrochemical reduction method employing a gold anode, a platinum cathode, and a silver plate [20]. The electrolytic solution of 6 mL containing 8.4 mM of hexadecyltrimethylammonium bromide (HMAB), purchased from Sigma-Aldrich and employed for the cationic surfactant, and 0.80 mM of tetraoctylammonium bromide (TOAB), purchased from Sigma-Aldrich and served for the cosurfactant, was added with 65 μ L of acetone and 45 μ L of cyclohexane. Electrolysis was performed with 5 mA for 10 min under continuous ultrasonication at 38 $^{\circ}$ C.

Gold colloidal solutions were dropped to amorphously carbon-coated copper grids and allowed for a day to dry at 50 $^{\circ}$ C in an oven for TEM examination using a microscope (JEOL, JEM-2000). Absorption spectra were obtained using a UV/vis spectrophotometer (Scinco, S-2040). Picosecond transient-absorption kinetic profiles were measured using an actively/passively mode-locked Nd:YAG laser (Quantel, YG701) of 25 ps and a streak camera (Hamamatsu, C2830) of 10 ps attached with a CCD detector (Princeton Instruments, RTE128H). Transient absorption produced by an excitation pulse of 532 nm having the spot diameter of 2 mm was probed with fluorescence, pseudo-CW in our dynamic range, from an organic dye. The dye was excited with a laser pulse split from the sample-excitation pulse. The comparison of dye-emission kinetic profiles with and without sample excitation yields a picosecond transient-absorption kinetic profile [21,22]. The wavelengths of probe light were selected by combining narrow-band and cut-off filters.

3 Results and discussion

Although aqueous gold nanorod colloids without being added with Cl^- do not (Fig. 1a), those with being added with Cl^- produce linearly aligned structures of linear bundles having long-range order after evaporation on a carbon-coated copper TEM grid (Figs. 1b–1d). This suggests that singly charged chloride ions induce gold nanorod colloids to flocculate into string-like aggregates. The magnified view of Figure 1d indicates that gold nanorods in the linear bundle of the mesoscopic scale are also oriented in nearly head-to-tail shapes in the microscopic scale. We infer that induced dipole-dipole long-range interactions of gold nanorods drive the aggregation process. The aggregation of nanorods is due to the inherently existing thermodynamic instability of nanoparticles in colloidal solutions. However, nanoparticles in colloidal solutions are suspended without being aggregated over indefinite time due to the repulsive interactions of their

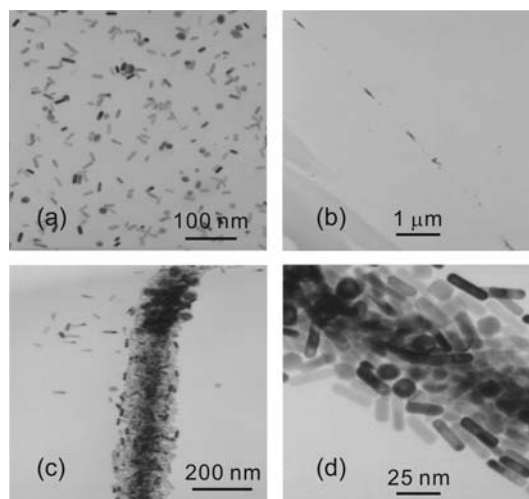


Fig. 1. TEM images of gold nanorods a day after dropping aqueous gold colloids without (a) and with NaCl of 0.63 mM (b–d) on carbon-coated copper TEM grids.

surface charges. Our synthesized nanorods also have partially positive surface charges due to the adsorption of not-completely reduced gold cations. Thus, the charged aggregants of chloride ions are assumed to assemble the nanomaterials by screening their partial surface charges. Highly concentrated and/or multiply charged ions produce tight aggregates showing ball-like structures while low concentrated and/or low charged aggregants lead to string-like aggregates [6]. However, the previously reported [6] aggregant-dependent formation of aggregates was observed microscopically with aggregated nanostructures having a dimension of just a few-hundred nanometers. In our nanorod study, the linear bundles of aggregates were linearly aligned in the mesoscopic scale and gold nanorods in aggregated bundles are also oriented in nearly head-to-tail shapes in the microscopic scale. The directional ordering of nanorods shown in Figure 1d can be explained by the distribution of partial surface charges in gold nanorods. Whereas surface charges in nanospheres are uniformly distributed within a nanosphere, those in nanorods are more likely divided in halves to locate at two ends. As anionic stabilizers are adsorbed to both ends, nanorods interact each other via induced dipoles to orient in head-to-tail structures.

The surface-plasmon absorption of gold nanorod colloids decreases at the transverse-mode band but increases at the longitudinal-mode band with Cl^- addition (Fig. 2). The peak positions are hardly changed while the bandwidths are slightly broadened with Cl^- addition. These suggest that the linear structures of aggregated gold nanorods are already produced in solutions with Cl^- addition although the linearity is extended further over the mesoscopic scale during evaporation on TEM grids. In the self-assembly of nanoparticles, the decrease of surface-plasmon absorption has been known to relate directly with the increase of the new absorption band in the vis/NIR region over 600 nm [6]. Then, the absorption changes with aggregation in our experiments are quite different from

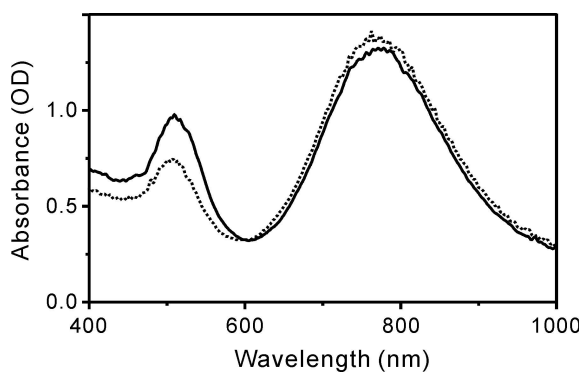


Fig. 2. Surface-plasmon absorption spectra of aqueous gold nanorod colloids without (solid) and with presence (dotted) of 5-mM HCl. The dotted one was taken 6 min after adding HCl.

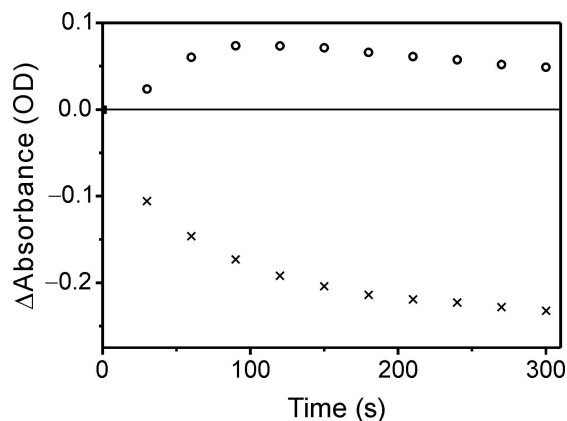


Fig. 3. Surface-plasmon absorbance changes of aqueous gold nanorod colloids monitored at 530 nm (crosses) and 720 nm (circles) with time after adding HCl to be 250 mM.

the reported ones [6]. Whereas the previous ones originate from the interparticle resonances of adjacent nanomaterials, ours from the oscillations of free electrons along the longitudinal axes of nanorods. Although the molar extinction coefficients of aggregated gold nanorods are not reported, it is reasonable to assume that the longitudinal extinction coefficient is much greater than the extinction coefficient of the new band arising from aggregates. Based upon this assumption, our observed absorption changes of Figure 2 can be understood. The spectral changes near the longitudinal resonances are not significant because the increase of interparticle absorption is compensated mostly by the longitudinal-absorption decrease of nanorods with aggregation.

Figure 3 shows that absorption at 530 nm decreases exponentially with time after Cl^- addition as the transverse resonances become weaker with the aggregation of nanorods. However, absorption variation monitored at 720 nm shows a complex feature having both rise and decay. As mentioned above, absorption above 600 nm in salt-added gold-nanorod colloids is composed of two different kinds of surface-plasmon resonances: one results from the longitudinal resonances of nanorods and the other

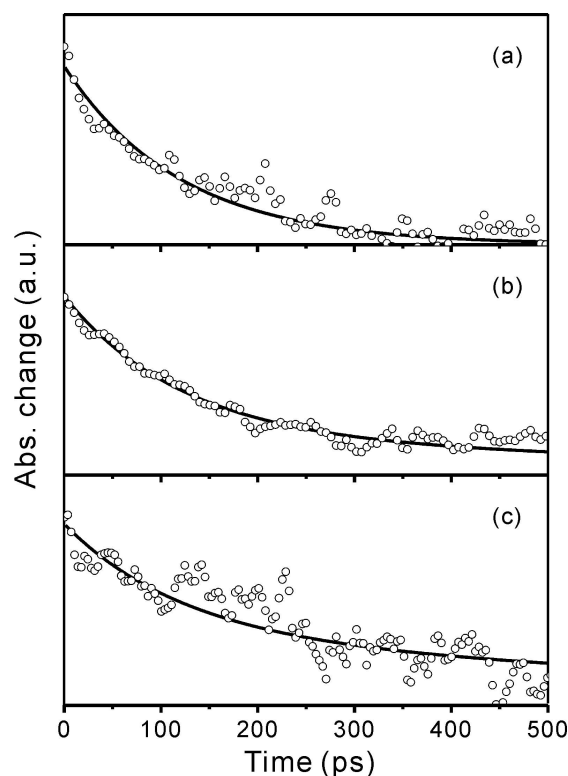


Fig. 4. Transient-absorption kinetic profiles, monitored at 620 nm after excitation at 532 nm, of aqueous gold nanorod colloids at the HCl concentrations of 0 (a), 5 (b), and 10 mM (c). Solid lines are best-fitted curves with kinetic constants given in Table 1.

Table 1. Decay times and initial fractional amplitudes of aqueous gold nanorod colloids, extracted from Figure 4.

kinetic curve	HCl (mM)	τ_1 (ps)	A_1	τ_2 (ps)	A_2
Fig. 4a	0	100	1.00		
Fig. 4b	5	100	0.78	800	0.22
Fig. 4c	10	100	0.60	800	0.40

from the interparticle resonances of aggregates. Thus, absorption at 720 nm increases with aggregation in the beginning as the new interparticle resonances are stronger in magnitude than the decrease of the longitudinal resonances. However, it decreases with further flocculation as the interior parts of aggregates cannot resonate with the incident light because of light scattering by large aggregates. Aggregation by an added salt is reported to take several minutes to a few weeks depending on the amount and the sort of the salt [5,6]. The continuing changes of absorption with time may signify the further growth of aggregates.

The transient absorption of gold nanorod colloids has a single-exponential decay time of 100 ps (Fig. 4 and Tab. 1), which is due to the heat dissipation via phonon-phonon interactions of noble-metal nanoparticles to immediately surrounding media [21]. A new component having a

slow-decay time of 800 ps increases with the concentration increase of HCl. This suggests that the heat dissipation of aggregates is much slower than that of dispersed nanorods. As gold nanoparticles having photon-thermalized heat interact with solvent molecules, coupling strength between surface phonons and solvent motions is suggested to determine the thermal-relaxation time of gold nanorods. Thus, the interparticle coupling in aggregates is so strong enough to slow down the thermal relaxation of a gold nanorod very significantly. Although the fractional amplitude increases with aggregation degree, the time constant of the slow component remains invariable, regardless of changes in the type and concentration of the aggregant as well as the time of aggregation. This suggests that our observed thermal relaxation time is an inherent character of gold nanorod aggregates.

In summary, aqueous gold nanorod colloids aggregated by Cl^- are further assembled into linearly aligned structures of linear bundles during evaporation on carbon-coated copper TEM grids. Gold nanorods in bundles are also oriented in nearly head-to-tail shapes in the microscopic scale. We suggest that induced dipole-dipole long-range interactions in the mesoscopic scale drive gold nanorods to aggregate. Whereas surface-plasmon absorption at transverse resonances decreases, that at longitudinal resonances increases with aggregation. Our transient-absorption study indicates that the photon-thermalized heat of the dispersed and the aggregated gold nanorods dissipates to immediately surrounding media on the time scales of 100 and 800 ps, respectively.

The Korea Research Foundation is appreciated for the grant of KRF-2003-041-C00151. D.-J.J. and O.-H.K. also acknowledge the Strategic National R&D Program (M1-0214-00-0108) and the Brain Korea 21, respectively.

References

1. Y. Yin, R.M. Rioux, C.K. Erdonmez, S. Hughes, G.A. Somorjai, A.P. Alivisatos, *Science* **304**, 711 (2004)
2. X.Y. Kong, Y. Ding, R. Yang, Z.L. Wang, *Science* **303**, 1348 (2004)
3. F. Yan, W.A. Goedel, *Nano Lett.* **4**, 1193 (2004)
4. J.-H. Choy, E.-S. Jang, J.-H. Won, J. H. Chung, D.-J. Jang, Y.-W. Kim, *Appl. Phys. Lett.* **84**, 287 (2004)
5. S. De, A. Pal, N.R. Jana, T. Pal, *J. Photochem. Photobiol. A* **131**, 111 (2000)
6. A.N. Shipway, M. Lahav, R. Gabai, I. Willner, *Langmuir* **16**, 8789 (2000)
7. M. Darder, E. Casero, D.J. Diaz, H.D. Abruna, F. Pariente, E. Lorenzo, *Langmuir* **16**, 9804 (2000)
8. C.G. Wing, P. Santiago, J.A. Ascencio, A. Camacho, M. Jose-Yacaman, *Appl. Phys. A* **71**, 237 (2000)
9. D. Lee, S. Lee, H. Kim, D.-J. Jang, *Eur. Phys. J. D* **24**, 303 (2003)
10. E.G. Timoshenko, R. Basovsky, Y.A. Kuznetsov, *Colloids Surf. A* **190**, 129 (2001)
11. T. Vossmeier, E. DeIonno, J.R. Heath, *Angew. Chem. Int. Ed. Engl.* **36**, 1080 (1997)
12. W.P. McConnel, J.P. Novak, L.C. Brousseau, R.R. Fuiierer, R.C. Tenent, D.L. Feldheim, *J. Phys. Chem. B* **104**, 8925 (2000)
13. A.A. Lazarides, K.L. Kelly, T.R. Jensen, G.C. Schatz, *J. Mol. Struct.* **529**, 59 (2000)
14. *Nanosystems, Molecular Machinery, Manufacturing and Computation*, edited by K.E. Drexler (Wiley, New York, 1992)
15. G. Schmid, *Chem. Rev.* **92**, 1709 (1992)
16. S.M. Marinakos, L.L. Brousseau, A. Jones, D.L. Feldheim, *Chem. Mater.* **10**, 1214 (1998)
17. A.P. Alivisatos, K.P. Johnsson, X. Peng, T.E. Wilson, C.J. Loweth, M.P. Bruchez, P.G. Schultz, *Nature* **382**, 609 (1996)
18. T.A. Taton, R.C. Mucic, C.A. Mirkin, R.L. Letsinger *J. Am. Chem. Soc.* **122**, 6305 (2000)
19. J.J. Storhoff, A.A. Lazarides, R.C. Mucic, C.A. Mirkin, R.L. Letsinger, G.C. Schatz, *J. Am. Chem. Soc.* **122**, 4640 (2000)
20. C.S. Ah, S.D. Hong, D.-J. Jang, *J. Phys. Chem. B* **105**, 7871 (2001)
21. C.S. Ah, H.S. Han, K. Kim, D.-J. Jang, *J. Phys. Chem. B* **104**, 8153 (2000)
22. S.J. Kim, T.G. Kim, C.S. Ah, K. Kim, D.-J. Jang, *J. Phys. Chem. B* **108**, 880 (2004)